Journal of Imaging Science and Technology® 51(4): 360–367, 2007.

Solving Under-Determined Models in Linear Spectral Unmixing of Satellite Images: *Mix-Unmix Concept* (Advance Report)

Thomas G. Ngigi and Ryutaro Tateishi
Center for Environmental Remote Sensing, Chiba University, 1-33 Yayoi, Inage, Chiba, 263-8522, Japan
E-mail: tgngigi@hotmail.com

Abstract. *This paper reports on a simple novel concept of addressing the problem of underdetermination in linear spectral unmixing. Most conventional unmixing techniques fix the number of end-members on the dimensionality of the data, and none of them can derive multiple (2^+) end-members from a single band. The concept overcomes the two limitations. Further, the concept creates a processing environment that allows any pixel to be unmixed without any sort of restrictions (e.g., minimum determinable fraction), impracticalities (e.g., negative fractions), or trade-offs (e.g., either positivity or unity sum) that may be associated with conventional unmixing techniques. The proposed mix-unmix concept is used to generate fraction images of four spectral classes from Landsat 7 ETM+ data (aggregately resampled to 240 m) first principal component only. The correlation coefficients of the mix-unmix image fractions versus reference image fractions of the four end-members are 0.88, 0.80, 0.67, and 0.78.* © *2007 Society for Imaging Science and Technology.*
[DOI: 10.2352/J.ImagingSci.Technol.(2007)51:4(360)]

PROBLEM STATEMENT / INTRODUCTION, AND OBJECTIVE

"*… the number of bands must be more than the number of end-members…*" is perhaps the most ubiquitous statement in the field of linear spectral unmixing. This is simply because most of the conventional unmixing techniques are based on least squares,[1] convex geometry,[2] or combination of both and the number of end-members (unknowns) is dependent on the dimensionality (equations) of the data. Least squares can unmix as many end-members as up to the dimensionality of the data, and at the very best exceed by one when the unity constraint is enforced. In convex geometry, the number of determinable end-members (at the unmixing stage) is equal to the number of vertices of the data simplex, and this number exceeds the dimensionality of the data by one. After extracting the end-member spectra, most of the convex geometry-based techniques apply the least squares approach (combined case) in computing the fractions of the end-members.

Some linear spectral unmixing techniques include Sequential Maximum Angle Convex Cone (SMACC) Spectral Tool,[3] (Generalized) Orthogonal Subspace Projection,[4,5] Convex Cone Analysis,[6] N-FINDR,[7] Orasis,[7] and Iterative Error Analysis.[7] Keshava[8] gives a detailed account of spectral unmixing techniques. A number of commercially available software, including ENVI, IDRISI Kilimanjaro, PCI, and ERDAS Imagine, have linear spectral unmixing modules. The greatest fundamental commonality of all conventional linear spectral unmixing techniques is that none of them can derive multiple end-members (2^+) from a single band. The object of the mix-unmix concept is to overcome this problem and unmix as many end-members as can be deciphered from the reference data and without introducing any sort of restrictions, impracticalities, or trade-offs that may be associated with conventional unmixing techniques.

DESCRIPTION OF THE MIX-UNMIX CONCEPT

As the term implies, the model consists of two branches, namely, mixing and unmixing. The mixing branch entails development of hypothetical mixed pixels on the basis of desired end-members' actual digital numbers (DNs). Unmixing involves determination of each real image pixel's DN's contributory end-members and their fractions by back-propagating through the mixing branch using a pixel of the same DN in the hypothetical image as a proxy. This preliminary study demonstrates the concept on a single simulated band.

Mixing Branch

Nominally, the end-members are paired up hierarchically into a single hypothetical mixed class (Figure 1; EM1 = end-member 1, EM1.2 = combined end-members 1 and 2). Essentially, in pairing up, each and every DN from a member of a pair is combined with each and every DN from the other member, at complementary percentages ranging from 0% to 100%, giving rise to various "mixture tables" (MTs) whose number depends on the ranges of training DNs of the two members.

Theory of the mixing branch and formation of mixture tables (MTs)

The number of possible DN combinations, MTs, of two members, A and B, of a pair is equal to the product of their training DN ranges, i.e.,

$$\text{MTs} = (\text{A max DN} - \text{A min DN} + 1) \times (\text{B max DN} - \text{B min DN} + 1),$$

where

Received Dec. 5, 2006; accepted for publication Mar. 22, 2007.
1062-3701/2007/51(4)/360/8/$20.00.

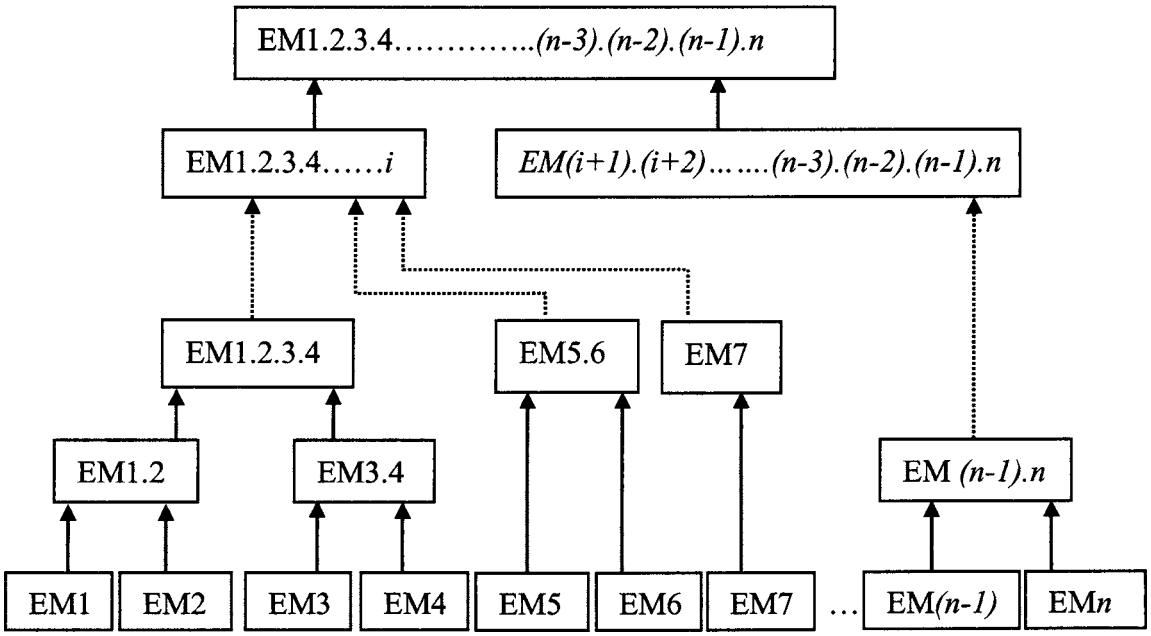

Figure 1. Bottom-up pairing up of end-members as well as the resultant super-end-members—pairing up involves mixing the two members-of-a-pair's DN ranges at all complementary fractions. In case the number of (super-)end-members is even but not a multiple of four, one level of mixing is skipped for one pair as indicated by EM5 and EM6 (for six end-members). For an odd number, one end-member is simply carried forward to the next level individually as indicated by EM7 (for seven end-members). In this case, EM5.6 and EM7 have the same hierarchical status as EM1.2.3.4. At the base of the branch are training DN ranges and assumed fractions of the end-members—the DNs are known by *in situ* observation, from spectral libraries, or identification of pure pixels in the image to be unmixed, etc. At the top of the branch are hypothetical pixels' DN values resulting from mixing all the end-members' spectra at all possible complementary fractions.

A max DN = maximum DN of A,

A min DN = minimum DN of A,

B max DN = maximum DN of B,

B min DN = minimum DN of B.

The number of possible percentages combinations, N%s, of the two members is given by

$$N\,\%\,s = (100\,\% \div MI) + 1,$$

where

MI = adopted mixture interval.

Subsequently, the total number of possible DNs and percentages combinations of the two is

$$MTs \times N\,\%\,s.$$

The expression also gives the total number of possible mixture pixels of the two.

Thus all pixels, in a hypothetical band, composed of only two end-members, EM1 and EM2, would be defined by the following expression—discussed assuming: that the end-members' training DNs range from, respectively, 10–89 and 90–150 in the band; a mixture interval of 10%, and assuming linear mixing.

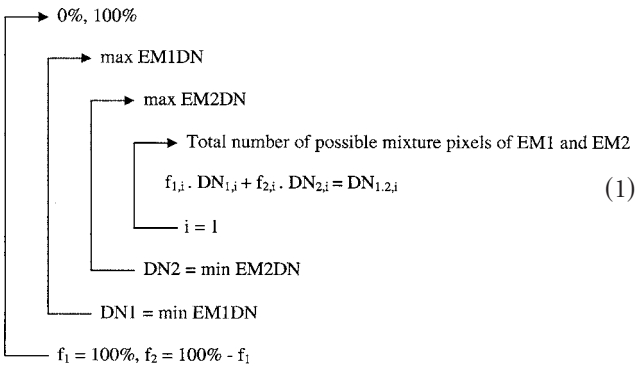

(1)

where

- $f_{1,i}$ = percentage of EM1 in pixel i [Table I(a) 1st column],
- $f_{2,i}$ = percentage of EM2 in pixel i [Table I(a) 2nd column],
- $f_1 + f_2 = 100\,\%$,
- $DN_{1,i}$ = DN of EM1 in pixel i [Table Ia 2nd row],
- $DN_{2,i}$ = DN of EM2 in pixel i [Table Ia 3rd row],
- $DN_{1,2,i}$ = mixture DN of $DN_{1,i}$ and $DN_{2,i}$ in pixel i [Table I(a) all cells excluding the first two columns and first three rows],

Table I. (a) MTs of EM1 and EM2. The EM1.2 DNs are computed as: EM1.2 DN = (EM1 % × EM1 DN) + (EM2 % × EM2 DN). Note that EM1% and EM2% are complementary.

	MT=	1	2	3–4 879	4 880	4 881
	EM1 DN=	10	11		88	89
	EM2 DN=	90	90		150	150
EM1%	EM2%	EM1.2 DN				
0	100	90	90		150	150
10	90	82	82		143	143
20	80	74	74		137	137
30	70	66	66		131	131
40	60	58	58		125	125
50	50	50	51		119	119
60	40	42	43		113	113
70	30	34	35		107	107
80	20	26	27		100	101
90	10	18	19		94	95
100	0	10	11		88	89

(b) Min-max MTs of EM1 and EM2.
(c) *Min-max LUTs of EM1 and EM2.*

		Min-MT EM1 DN = 10 EM2 DN = 90 *Min-LUT*	Max-MT EM1 DN = 89 EM2 DN = 150 *Max-LUT*	
EM1 %	EM2 %	EM1.2 DN		*Amount of overlap with EM1.2 vector (90–150)*
0	100	90	150	*60*
10	90	82	143	*53*
20	80	74	137	*47*
30	70	66	131	*41*
40	60	58	125	*35*
50	50	50	119	*29*
60	40	42	113	*23*
70	30	34	107	*17*
80	20	26	101	*11*
90	10	18	95	*5*
100	0	10	89	*0*

- min EM1DN = minimum DN of EM1,
- max EM1DN = maximum DN of EM1.

Bounding mixture tables, and various numbers of end-members

From Table I(a), it is very clear that, given constant fractions of EM1 and EM2, the mixture class DNs (EM1.2 DNs) always fall between the values in the first and last MTs, thus the two MTs fully give the ranges of all possible DNs of EM1.2. Hereinafter, the two are referred to as min-MT and max-MT, respectively, and min-max MTs collectively [Table I(b)].

Similarly, min-max MTs of the other paired end-members are generated: for EM3 and EM4; in Eq. (1) EM1, EM2, and EM1.2 are replaced with EM3, EM4, and EM3.4, respectively. Table II(a) shows min-max MTs of EM3 and EM4 shows the DN ranges are 151–180 and 181–210, respectively.

Next, second level min-max MTs are developed from the above first level MTs: for EM1.2 and EM3.4; in Eq. (1) EM1, EM2, and EM1.2 are replaced with EM1.2, EM3.4, and EM1.2.3.4, respectively. Table III(a) shows min-max MTs of EM1.2, and EM3.4. Since EM1.2 represents EM1 and EM2, and EM3.4 represents EM3 and EM4, subsequently, the second level min-max MTs inherently represent all the possible DN outcomes of mixing all the end-members EM1, EM2, EM3, and EM4 at all possible complementary fractions.

Table II. (a) Min-max MTs of EM3 and EM4. The EM3.4 DNs are computed as: EM3.4 DN = (EM3% × EM3 DN) + (EM4% × EM4 DN). Note that EM3% and EM4% are complementary. (*b*) *Min-max LUTs of EM3 and EM4.*

		Min-MT EM3 DN = 151 EM4 DN = 181 *Min-LUT*	Max-MT EM3 DN = 180 EM4 DN = 210 *Max-LUT*	*Amount of overlap with EM3.4 vector 172–201*
EM3 %	EM4 %	EM3.4 DN		
0	100	181	210	*20*
10	90	178	207	*29*
20	80	175	204	*29*
30	70	172	201	*29*
40	60	169	198	*26*
50	50	166	195	*23*
60	40	163	192	*20*
70	30	160	189	*17*
80	20	157	186	*14*
90	10	154	183	*11*
100	0	151	180	*8*

For more end-members, the process is successively repeated as shown in Fig. 1. For three end-members in Eq. (1) EM1, EM2, and EM1.2 are replaced with EM1.2, EM3, and EM1.2.3, respectively.

Unmixing Branch

This is similar to the mixing branch (Fig. 1) but with the arrows (processing) reversed and the MTs renamed look-up-tables (LUTs)—Tables I(c), II(b), and IIIb. As discussed below, a real image pixel DN is fractionalized into two highest level super-end-members, each of which is then split into its two constituent end-members. The process continues until the finest level (end-members of interest) from which the mixing branch was constructed (see Figure 2).

Fractionalization

This discussion demonstrates the unmixing process on a single-band image composed of the four end-members outlined in the Mixing Branch section. For each DN in the band, all the vectors in which it lies are identified, e.g., Table III(b) EM.1.2.3.4 italicized DNs give all the possible vectors for DN 180, with the lower nodes located in Table III(b-1) and the upper nodes in Table III(b-2)—the first vector is 172–204 (bold). Each one of these vectors is a combination of two minor vectors, one apiece from EM1.2 and EM3.4 (italicized); e.g., for the vector 172–204, the constituent vectors are 90–150 (bold) from EM1.2 and 181–210 (bold) from EM3.4.

The most probable vector (MPV) in which the DN 180 lies is computed as

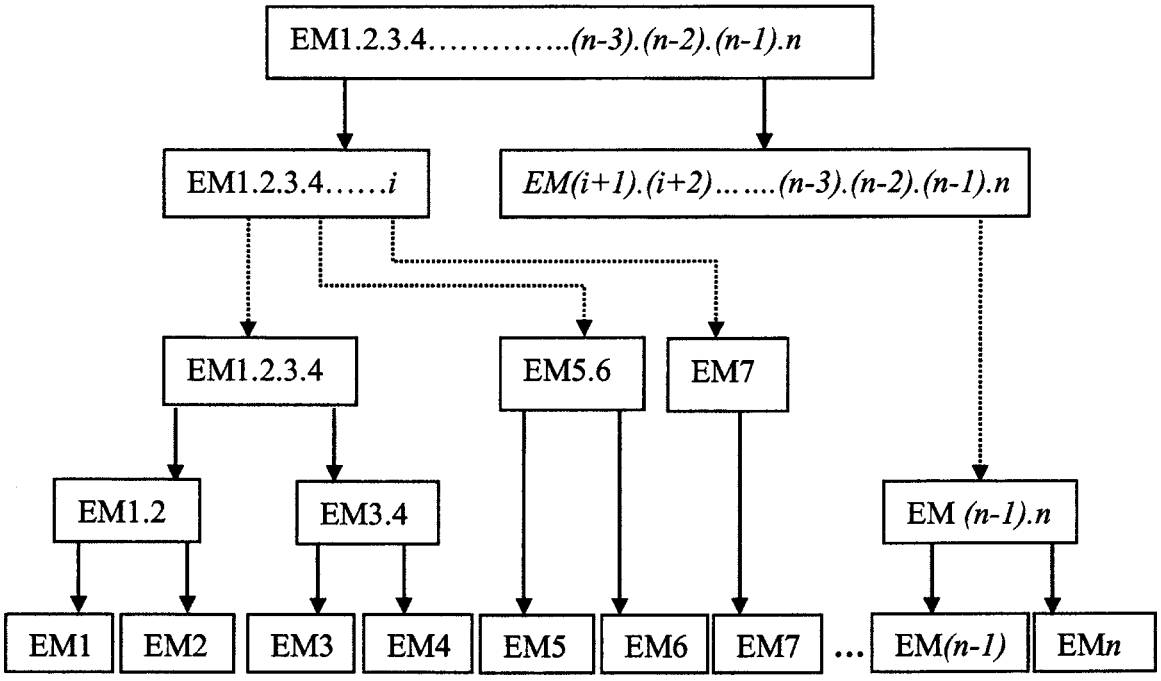

Figure 2. Top-bottom fractionalization of a pixel; first into two highest level super-end-members, then effectively into second highest level four super-end-members by fractionalizing each of the highest level super-end-members into two. The process is repeated successively until the lowest level end-members that were used to build up the mixing branch. At the top of the branch is a universe of values encompassing *all* the DNs in the image to be unmixed—*all*: assuming that the image is composed of only the end-members used in the mixing branch. At the base of the branch are estimated contributory percentages (fractions) of the end-members (cf. Fig. 1).

Table III. (a-1) Min-MT of EM1.2 and EM3.4. The EM1.2.3.4 DNs are computed as: EM1.2.3.4 DN = (EM1.2% × EM1.2 DN) + (EM3.4% × EM3.4 DN). Note that EM1.2% and EM3.4% are complementary. (*b-1*) *Min-LUT of EM1.2 and EM3.4.*

			EM3.4 DN[b]										
EM1.2 DN[a]	EM1.2 %	EM3.4 %	***181***	*178*	*175*	*172*	*169*	*166*	*163*	*160*	*157*	*154*	*151*
								EM1.2.3.4 DN					
90	0	100	181	*178*	*175*	*172*	*169*	*166*	*163*	*160*	*157*	*154*	*151*
90	10	90	***172***	*169*	*167*	*164*	*161*	*158*	*156*	*153*	*150*	*148*	145
90	20	80	*163*	*160*	*158*	**156**	*153*	*151*	*148*	*146*	144	141	139
90	30	70	*154*	*152*	*150*	*147*	*145*	*143*	141	139	137	135	133
90	40	60	*145*	*143*	*141*	*139*	137	136	134	132	130	128	127
90	50	50	*136*	134	133	131	130	128	127	125	124	122	121
90	60	40	126	125	124	123	122	120	119	118	117	116	114
Rows 8 to 117													
10	70	30	61	60	60	59	58	57	56	55	54	53	52
10	80	20	44	44	43	42	42	41	41	40	39	39	38
10	90	10	27	27	27	26	26	26	25	25	25	24	24
10	100	0	10	10	10	10	10	10	10	10	10	10	10

(a-2) Max-MT of EM1.2 and EM3.4.
(*b-2*) *Max-LUT of EM1.2 and EM3.4.*

			EM3.4 DN[d]										
EM1.2 DN[c]	EM1.2 %	EM3.4 %	***210***	*207*	*204*	*201*	*198*	*195*	*192*	*189*	*186*	*183*	*180*
								EM1.2.3.4 DN					
150	0	100	210	*207*	*204*	*201*	*198*	*195*	*192*	*189*	*186*	*183*	*180*
150	10	90	***204***	*201*	*199*	*196*	*193*	*191*	*188*	*185*	*182*	*180*	177
150	20	80	*198*	*196*	*193*	**191**	*188*	*186*	*184*	*181*	179	176	174
150	30	70	*192*	*190*	*188*	*186*	*184*	*182*	179	177	175	173	171
150	40	60	*186*	*184*	*182*	*181*	179	177	175	173	172	170	168
150	50	50	*180*	179	177	176	174	173	171	170	168	167	165
150	60	40	174	173	172	170	169	168	167	166	164	163	162
Rows 8 to 117													
89	70	30	125	124	124	123	122	121	120	119	118	117	116
89	80	20	113	113	112	111	111	110	110	109	108	108	107
89	90	10	101	101	100	100	100	99	99	99	99	98	98
89	100	0	89	89	89	89	89	89	89	89	89	89	89

[a]Column 1 elements are from EM1 and EM2 min-MT [Table I(b), column 3]
[b]Row 1 elements are from EM3 and EM4 min-MT [Table IIa, column 3]
[c]Column 1 elements are from EM1 and EM2 max-MT [Table I(b), column 4]
[d]Row 1 elements are from EM3 and EM4 max-MT [Table IIa, column 4]

$$\text{cMNxDN} = \frac{\sum_{i=1}^{n} \text{lower\_nodes}}{n}, \tag{2}$$

$$\text{cMNyDN} = \frac{\sum_{i=1}^{n} \text{upper\_nodes}}{n}, \tag{3}$$

where

- cMNxDN = lower node of DN 180 MPV from combined classes M and N (EM1.2 or EM3.4),
- cMNyDN = upper node ditto,
- lower nodes = all the EM1.2.3.4 italicized DN in Table III(b-1),
- upper nodes = ditto Table III(b-2),
- n = number of EM1.2.3.4 italicized DN vectors = count of EM1.2.3.4 italicized DN nodes in Table III(b-1) or Table III(b-2).

From Eqs. (2) and (3), *cMNxDN* = 156 and *cMNyDN* = 190. From Table III(b), the pair of nodes most close to the pair 156/190 is 156/191 and it is adopted as the MPV for the DN 180. This vector 156–191 [Table III(b) bold and underlined] lies at the intersection of EM1.2 vector 90–150

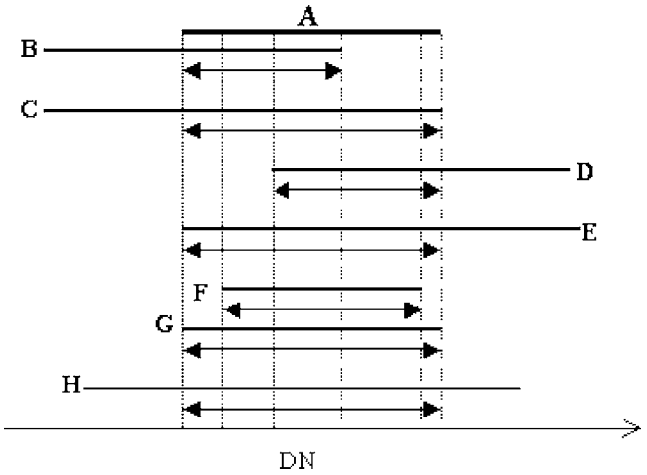

Figure 3. Possible universal overlap scenarios. A is EMx.y's most probable vector, e.g., EM1.2 MPV 90-150 or EM3.4 MPV 172-201; all/some of the other non-arrowed lines (B-H) are vectors contained in EMx.y's min-max LUTs [e.g., Table I(c) for EM1.2, or Table II(b) for EM3.4]; arrowed lines are the respective overlaps.

and EM3.4 vector 172–201. Therefore, by extension, the DN 180 most probably resulted from these EM1.2 and EM3.4 vectors as the combination most probably gave rise to the DN 180 MPV 156–191.

Further, percentages-wise, the DN 180 could have resulted from any of the paired percentages associated with the EM1.2.3.4 italicized DNs vectors. The most probable contributory paired percentages (MPPC) are computed as

$$MPPC_{x.y} = \frac{\sum_{i=1}^{n} (i\%_{x.y} \times p_i)}{n\sum_{i=1}^{n} p_i} \pm \sqrt{\frac{\sum_{i=1}^{n} p_i v_i^2}{n^2 \sum_{i=1}^{n} p_i}}, \qquad (4)$$

where

- $i\%_{x.y}$ = ith paired percentages of x (EM1.2) and y (EM3.4),
- p_i = weight of $i\%_{x.y}$ = count of $i\%_{x.y}$'s EM1.2.3.4 italicized DNs,
- n = count of probable contributory paired percentages,
- $v = i\%_{x.y} - \mathrm{MPPC}_{x,y}$. The second term in Eq. (4) is computed after the first one.

From Eq. (4), EM1.2% = 16.67% ± 2.34% and EM3.4% = 83.33% ± 2.34%. Hence, the DN 180 most probably resulted from these EM1.2 and EM3.4 percentages combinations as the pair most probably gave rise to the DN 180 MPV 156-191.

Next, the EM1.2 90-150 and EM3.4 172-201 vectors are checked against the lower level min-max LUTs, Tables I(c) and II(b), respectively, and all the vectors with which they (EM1.2 and EM3.4 vectors) overlap form the universe of possible vectors (PVs) from which they (EM1.2 and EM3.4 vectors) or, in other words, a fraction of the value 180, arose. The probability (weight) of each of the Table I(c) PVs having given rise to the EM1.2 vector 90–150 is taken to be proportional to the amount of overlap with it. Each probability is also taken to be the probability of the corresponding paired percentages (PPs) having given rise to the EM1.2 vector 90–150 since the PV was developed from them (PPs). Similarly for Table II(b) PVs and PPs in the case of EM3.4 vector 172–201. There are seven possible overlap scenarios as depicted by Figure 3. Table I(c) last column gives the weights of the EM1 and EM2 vectors to EM1.2 vector 90–150, and Table II(b) ditto EM3 and EM4 vectors to EM3.4 vector 172–201.

From Fig. 3 and Tables I(c) and II(b), the most probable percentage contribution (MPPC) of each daughter class to its mother class is computed as

$$cM\% = \frac{\sum_{i=1}^{q} cM\%_i \times p_i}{q\sum_{i=1}^{q} p_i} \pm \sqrt{\frac{\sum_{i=1}^{q} p_i v_i^2}{q^2 \sum_{i=1}^{q} p_i}}, \qquad (5)$$

where

- $cM\%$ = MPPC of daughter class cM (EM1 or EM2) to its mother class (EM1.2). EM3 or EM4 for EM3.4;
- $cM\%_i$ = percent of cM's ith probable vector—Table I(c) columns 1 and 2 for EM1 and EM2, respectively; Table II(b) columns 1 and 2 for EM3 and EM4, respectively;
- p_i = overlap range of cM's ith probable vector with its (cM) mother's MPV. Table I(c) last column for EM1 and EM2. Table II(b) last column for EM3 and EM4;
- q = count of probable paired-percentages;
- $v = cM\% - cM\%_i$. The second term in Eq. (5) is computed after the first one.

From Eq. (5) and Tables I(c) and II(b), the MPPCs of EM1 and EM2 to EM1.2, and EM3 and EM4 to EM3.4 are; EM1 = 71% ± 2.84%, EM2 = 29% ± 2.84%, EM3 = 59% ± 2.42%, and EM4 = 41% ± 2.42%.

The MPPC of an end-member to the original pixel DN is simply the product of all MPPCs along the path from the end-member itself to the pixel DN. Hence, for end-member:

- 1 = EM1% × EM1.2% = 71% × 16.67% = 11.84 ± 1.73%,
- 2 = EM2% × EM1.2% = 29% × 16.67% = 04.83 ± 0.83%,
- 3 = EM3% × EM3.4% = 59% × 83.33% = 49.16 ± 2.44%,
- 4 = EM4% × EM3.4% = 41% × 83.33% = 34.17 ± 2.23%.

The standard deviation of product AB is computed as

$$\sigma_{AB} = AB\sqrt{\left(\frac{\sigma_A}{A}\right)^2 + \left(\frac{\sigma_B}{B}\right)^2}, \qquad (6)$$

where σ_k = standard deviation of k.

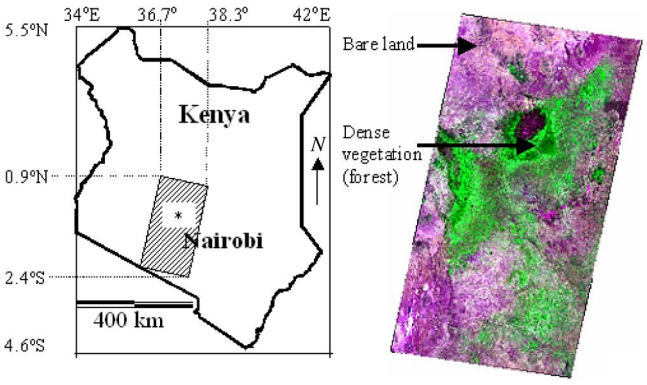

Figure 4. (Left) location of the study area; (right) 30 m resolution Landsat ETM+ data RGB=342.

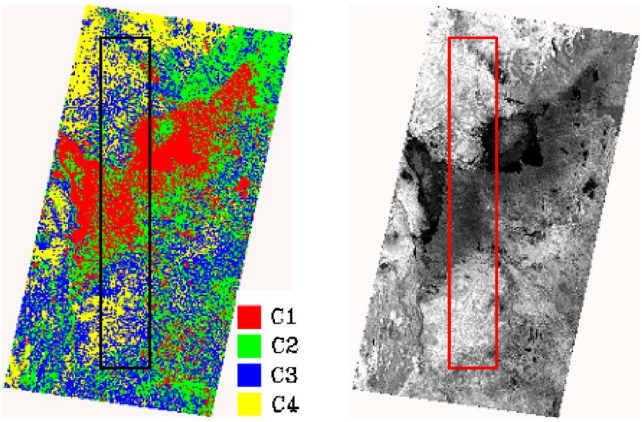

Figure 5. (Left) reference data: 30 m resolution spectral classes. The spectral classes correspond to broad information classes dense vegetation (C1), dense vegetation/bare land (C2), bare land/dense vegetation (C3), and bare land (C4); (right) raw image: 240 m resolution first principal component. The rectangles show locations of reference (black) and mix-unmix (red) training sites.

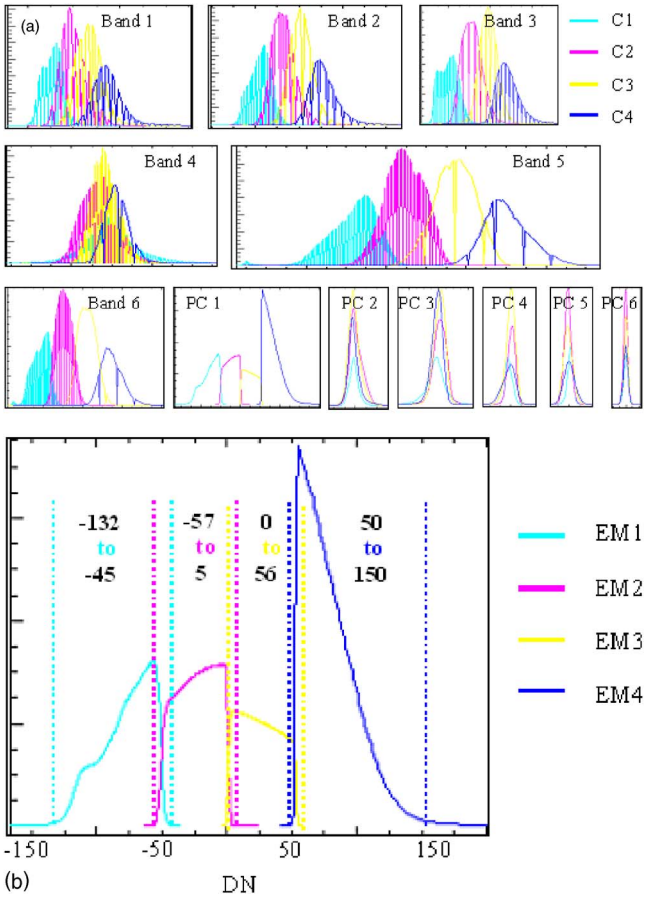

Figure 6. (a) Comparison of DNs' distribution curves of C1, C2, C3, and C4 in mix-unmix training site across original bands and principal components (PCs). The least overlap between the curves occurs in PC1 and, thus, it is adopted as the raw band to unmix. Y axes=frequencies, and X axes=DNs—but values not shown. (b) Training DNs of EM1, EM2, EM3, and EM4.

STUDY TEST

Four spectral end-members are mapped from a single-band simulated raw image.

Study Area and Data

Landsat ETM+ data, of 21 February 2000, covering southern-central Kenya is utilized to generate both the reference and raw data. The land covers in the area transition from dense vegetation (forest) to bare land (Figure 4).

Simulation of Reference and Raw Data

K-mean classification is run on the ETM+ data bands 1, 2, 3, 4, 5, and 7 to produce four spectral classes. The spectral classes are adopted as reference data. The six bands data is resampled to 240 m resolution (mimics moderate resolution data, e.g., MODIS bands 1 and 2–250 m resolution) and then principal components transformation (PCT) executed on the new data set. Each of the resampled bands and PCs is taken as a candidate raw image.

Selection of Band to Unmix, and its Unmixing

A section from the 30 m resolution reference spectral classes image, black rectangle in Figure 5, hereinafter referred to as reference training site, is geographically overlaid on each candidate raw image (240 m resolution) and pure pixels in the overlay section, red rectangle in Fig. 5, hereinafter referred to as mix-unmix training site, of the candidate raw image for each spectral class identified. A pixel in the mix-unmix training site is pure if the geographically corresponding 8-pixel×8-pixel block in the reference training site is composed of a single class, 8 is the ratio of the two resolutions. Figure 6(a) compares the four spectral classes' pure-pixels' DNs' distribution curves in the mix-unmix training site. Since the four spectral classes exhibit the highest spectral dissimilarity between themselves in the first PC, it is adopted as the raw image to be unmixed. The training DN ranges of the four spectral classes (now denoted as end-members, EMs) are as shown in Fig. 6(b). The raw image (first PC) is unmixed under the mix-unmix concept on the basis of the training DNs into the four end-members.

Mix-Unmix Fraction Images versus Reference Fraction Images

Reference fraction images of the four spectral classes (Fig. 5) are generated by computing the percentage coverage of each class in every 8-pixel×8-pixel block (each block is 240 m

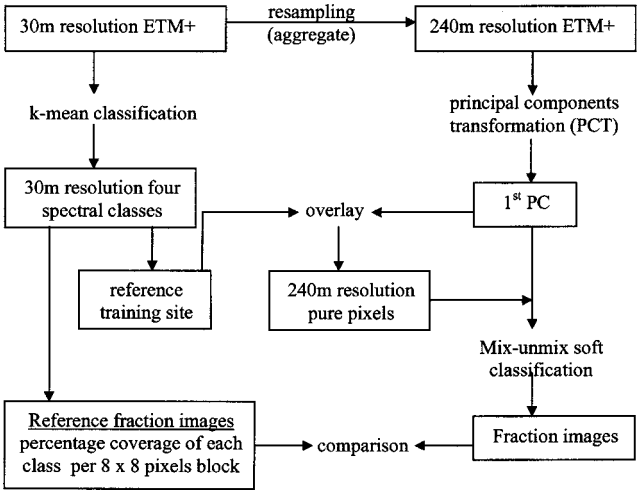

Figure 7. Data processing flowchart.

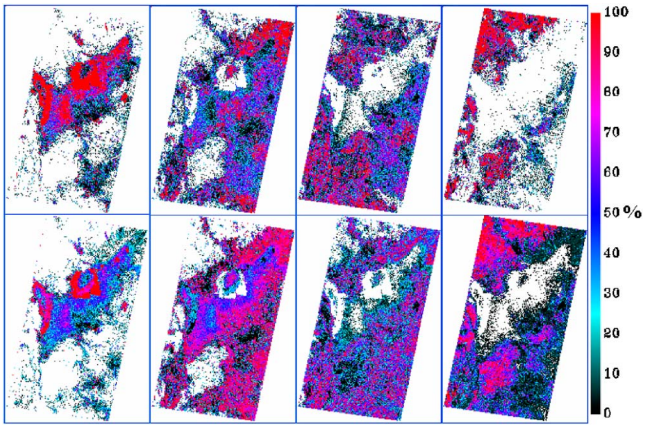

Figure 8. Reference fraction images (upper row) and Mix-unmix fraction images (lower row) of four end-members (first column=EM1, second =EM2, third=EM3, fourth=EM4). White and black are background, i.e., 0%.

×240 m). The reference fraction images are compared with the mix-unmix fraction images. Figure 7 outlines the entire image processing flow, and Figure 8 compares the fraction images. The correlation coefficients of the mix-unmix image fractions versus the reference image fractions of the four end-members are 0.88 (EM1), 0.80 (EM2), 0.67 (EM3), and 0.78 (EM4).

DISCUSSION

The mix-unmix fraction images show similar transition patterns (highest to lowest concentration levels) as the reference fraction images for all the end-members; though the correlation coefficients are not "very high." Although a mixture interval of 10% is used throughout this study, any value that as a divisor of 100 gives a whole number can be used. We cannot use 100 itself as it would mean that each pixel contains just a single end-member.

FUTURE

As discussed in the Mixing Branch section, only the extreme DN values (i.e., bounding mixture tables) are used in this study. Also, the training DNs of end-members are assumed to be "frequency-less." As the mix-unmix software develops, all mixture tables and training DNs' distribution curves will be incorporated.

The effect of adopted mixture interval and overlap of training DNs on accuracy of the concept will be addressed on implementation of the above. Also, performance of the concept across different numbers of end-members, different resolutions, and different geographical scales will be tested.

CONCLUSIONS

This preliminary investigation shows that the mix-unmix concept is capable of addressing the problem of under-determination in linear spectral unmixing—a very revolutionary dimension in data processing as the number of end-members is not pegged on that of available bands. It is the only method that truly solves the problem of under-determination. Sequential Maximum Angle Convex Cone (SMACC) Spectral Tool does not work on a single band, and Generalized Orthogonal Subspace Projection cannot generate additional bands from a single band. Further, the mix-unmix concept creates a processing environment that allows any pixel to be unmixed without any sort of restrictions (e.g., minimum determinable fraction), impracticalities (e.g., negative fractions), or trade-offs (e.g., either positivity or unity sum) that may be associated with conventional unmixing techniques.

REFERENCES

[1] Y. E. Shimabukuro and J. A. Smith, "The least squares mixing methods to generate fraction images derived from remote sensing multispectral data", IEEE Trans. Geosci. Remote Sens. **29**, 16 (1991).
[2] J. W. Boardman, "Geometric mixture analysis of imaging spectrometry data", *Proc. Int. Geosci Remote Sens Symposium* **4**, 2369 (1994).
[3] J. Gruninger, A. J. Ratkowski, and M. L. Hoke, "The sequential maximum angle convex cone (SMACC) endmember model", Proc. SPIE **5425** 1 (2004).
[4] R. Hsuan and C. Yang-Lang, "Error Analysis for Band Generation in Generalized Process Orthogonal Subspace Projection", *IEEE Geoscience and Remote Sensing Symposium Proceedings, IGARSS* (IEEE Press, Piscataway, NJ, 2005).
[5] I. Emmett, "Hyperspectral Image Classification Using Orthogonal Subspace Projections: Image Simulation and Noise Analysis", http://www.cis.rit.edu/~ejipci/Reports/osp_paper.pdf (2001).
[6] A. Ifarraguerri and C. Chang, "Multispectral and Hyperspectral Image Analysis with Convex Cones", IEEE Trans. Geosci. Remote Sens. **37**, 756 (1999).
[7] M. E. Winter and E. M. Winter, "Comparison of approaches for determining end-members in hyperspectral data", *Proc. IEEE Aerospace Conference* (IEEE Press, Piscataway, NJ, 2000).
[8] N. Keshava, "A Survey of Spectral Unmixing Techniques", Lincoln Lab. J. **14**, 55 (2003).